mathematics

MDPI

Article

Bifurcation of an SIRS Model with a Modified Nonlinear Incidence Rate

Yingying Zhang [1,*] and Chentong Li [2]

[1] College of Science, Northwest A&F University, Yangling 712100, China
[2] Guangdong Key Laboratory of Mordern Control Technology, Institute of Intelligent Manufacturing, Guangdong Academy of Sicence, Guangzhou 510070, China; ct.li@giim.ac.cn
* Correspondence: zyy0303@nwafu.edu.cn

Abstract: An SIRS epidemic model with a modified nonlinear incidence rate is studied, which describes that the infectivity is strong at first as the emergence of a new disease or the reemergence of an old disease, but then the psychological effect will weaken the infectivity. Lastly, the infectivity goes to a saturation state as a result of a crowding effect. The nonlinearity of the functional form of the incidence of infection is modified, which is more reasonable biologically. We analyze the stability of the associated equilibria, and the basic reproduction number and the critical value which determine the dynamics of the model are derived. The bifurcation analysis is presented, including backward bifurcation, saddle-node bifurcation, Bogdanov–Takens bifurcation of codimension two and Hopf bifurcation. To study Hopf bifurcation of codimension three of the model when some assumptions hold, the focus values are calculated. Numerical simulations are shown to verify our results.

Keywords: SIRS model; backward bifurcation; saddle-node bifurcation; Bogdanov–Takens bifurcation; Hopf bifurcation

MSC: 34C23

Citation: Zhang, Y.; Li, C. Bifurcation of an SIRS Model with a Modified Nonlinear Incidence Rate. *Mathematics* **2023**, *11*, 2916. https://doi.org/10.3390/math11132916

Academic Editors: Biao Tang and Xia Wang

Received: 24 May 2023
Revised: 12 June 2023
Accepted: 18 June 2023
Published: 29 June 2023

1. Introduction

In epidemiology modeling, there are several factors that substantially affect the dynamical behavior of the models. Therein, the incidence rate is very crucial for describing the spreading of disease; in general, some nonlinear incidence rates play key roles in producing the rich dynamics, including bistability (backward bifurcation) and periodicity [1–5]. The general incidence rate $kI^pS/(1+\alpha I^q)$ $(q = p-1)$ was investigated by Liu et al. [6,7]. Hethcote and van den Driessche [8] considered the case $p \geq q$. Tang et al. [9] and Hu et al. [10] proposed that the incidence function $kI^p/(1+\alpha I^q)$ with respect to I, which measures the infection force of a disease, includes three cases: (I) if $p < q$, it is unbounded; (II) if $p = q$, it is saturated; (III) if $p < q$, it is nonmonotone. the first case may be true in the early process of the disease or the number of the infective individuals $I(t)$ is small, but will become unrealistic when $I(t)$ is getting larger.

In the second scenario, considering the inhibitory effect from the behavioral change of the susceptible individuals when the number of infective individuals increases, Ruan and Wang [4] studied a model with a saturated nonlinear incidence rate $kI^2S/(1+\alpha I^2)$, where kI^2 measures the infection force of the disease and $1/(1+\alpha I^2)$ describes the inhibitory effect, and they investigated the global dynamics of the model. The incidence function $kI^2/(1+\alpha I^2)$ monotonously and eventually goes to a saturation level $\frac{k}{\alpha}$ as I becomes larger. However, when a new infectious disease emerges which people know little about and to which they are caught off guard, the infection force of the disease increases rapidly until the disease attracts people's attention, and they will change their behaviors, such as giving up risky behavior or taking precautionary measures to reduce the transmission, and then, the infection force will decrease. This is the psychological effect. The outbreak of

2019 novel coronavirus diseases (COVID-19) in Wuhan, Hubei Province, China, showed such psychological effects on the general public, including aggressive measures and policies, such as rapid isolation of suspected cases, confirmed cases, and contacts; restrictions on mobility; travel restrictions; keeping distance from others; mask-wearing; etc., was clearly successful in mitigating spread and reducing the local transmission of COVID-19 in China [11–13]. Similarly, in the epidemic outbreak of severe acute respiratory syndrome (SARS) in 2003 [14], these measures, including border screening, mask-wearing [15], quarantine [16], isolation, etc., proved to be effective in reducing the spread of SARS. Obviously, the monotone incidence rates may not be used to describe the psychological effect perfectly. Xiao and Ruan [17] proposed an epidemic model with incidence $kIS/(1+\alpha I^2)$ to model the effect and carried out a global analysis of the model and showed that either the number of infective individuals tends to zero as time evolves or the disease persists. The dynamics of this model was relatively simple.

Xiao and Zhou [18] and Zhou et al. [19] studied an epidemic model with the nonmonotonic incidence rate of saturated mass action $kIS/(1+\beta I+\alpha I^2)$, and Xiao and Zhou carried out a global analysis and showed the existence of bistability and periodicity. Zhou et al. presented the bifurcation analysis of the model, such as Hopf bifurcation and Bogdanov–Takens bifurcation. Both nonmonotonic and saturated incidence functions $kI/(1+\alpha I^2)$ and $kI/(1+\beta I+\alpha I^2)$ approach zero when I tends to infinite, which implies that the psychological or inhibitory effect is so strong that the disease incidence becomes zero, which may be unreasonable for some diseases, such as influenza. Considering a more reasonable incidence function which goes up at first at the onset of a disease, then goes down because of the psychological effect, and goes to a saturation level at length due to the crowding effect, Lu et al. [20] proposed a generalized nonmonotone and saturated incidence rate $kI^2S/(1+\beta I+\alpha I^2)$, where parameter $\beta > -2\sqrt{\alpha}$ to make $1+\beta I+\alpha I^2 > 0$ hold for all $I \geq 0$, and when $\beta \geq 0$, the incidence function $kI^2/(1+\beta I+\alpha I^2)$ increases monotonously to a saturated level $\frac{k}{\alpha}$ as I goes to infinite. When $-2\sqrt{\alpha} < \beta < 0$, $kI^2/(1+\beta I+\alpha I^2)$ is nonmonntonic, which grows at first and then descends to a saturated level $\frac{k}{\alpha}$ as $I \to \infty$. They studied the following model with this incidence rate and found that the model showed rich dynamical behaviors, including saddle-node bifurcation, Bogdanov–Takens bifurcation of codimension two, and degenerate Hopf bifurcation of codimension two.

$$\begin{cases} \dfrac{dS}{dt} = b - dS - \dfrac{kI^2}{1+\beta I+\alpha I^2}S + \nu R, \\ \dfrac{dI}{dt} = \dfrac{kI^2}{1+\beta I+\alpha I^2}S - (d+\gamma)I, \\ \dfrac{dR}{dt} = \gamma I - (d+\nu)R. \end{cases} \tag{1}$$

where S represents susceptible compartment, I represents infective compartment, and R represents recovered compartment. All parameters except β are positive in the model. Here, b is the natural birth rate, d is the natural death rate, μ is the recovery rate, k is the infection rate, and α describes the psychological effect. Recovered individuals lose immunity and move into susceptible compartment S at rate ν.

The basic reproduction number R_0 is the single most important parameter in epidemic modeling, which measures the average number of secondary infections caused by a single infectious individual in an entirely susceptible population during the mean infectious period [21]. The incidence rate $kI^2S/(1+\beta I+\alpha I^2)$, with combination of monotonicity, nonmonotonicity, and saturation properties, seems reasonable to describe the transmission process of some specific infectious diseases. In fact, the basic reproduction number of model (1) with the incidence rate is zero, but they proved that the disease still persisted for some parameters and initial conditions, which seems unreasonable. Moreover, the parameter β can take a negative value and does not have a realistic biological meaning, and it may seem be farfetched to endow the incidence rate with the combination of monotonicity,

nonmonotonicity, and saturation properties. Hence, by the above analysis, we propose a more reasonable incidence rate:

$$f(I)S = \frac{k_1 I + k_2 I^2}{1 + \alpha I^2} S,$$

where the incidence function $f(I) = \frac{k_1 I + k_2 I^2}{1+\alpha I^2}$ reserves the combination of monotonicity, nonmonotonicity, and saturation properties, i.e., when $k_1 = 0$, $f(I)$ increases monotonously to a saturated level $\frac{k_2}{\alpha}$ as I goes to infinite; when $k_1 > 0$, $f(I)$ is nonmonntonic, which increases at first and then decreases to a saturated level $\frac{k_2}{\alpha}$ as I tends to infinite (see Figure 1). Moreover, the basic reproduction number and all parameters have biological meaning with reasonable explanation. Moreover, this incidence rate enriches the model with more rich dynamical behaviors. In fact, in 2000, an epidemic model with the incidence rate $(k_1 I + k_2 I^2)S$ was proposed by P. van den Driessche et al. [2], considering the contact rate may depend on the fraction of infective individuals or on the severity of infection in the infected individual, and Li et al., 2007 [22] and Li et al., 2014 [23] presented that the model showed very rich dynamical behaviors, including backward bifurcation, the Hopf bifurcation and Bogdanov–Takens bifurcation, and canard phenomenon, respectively.

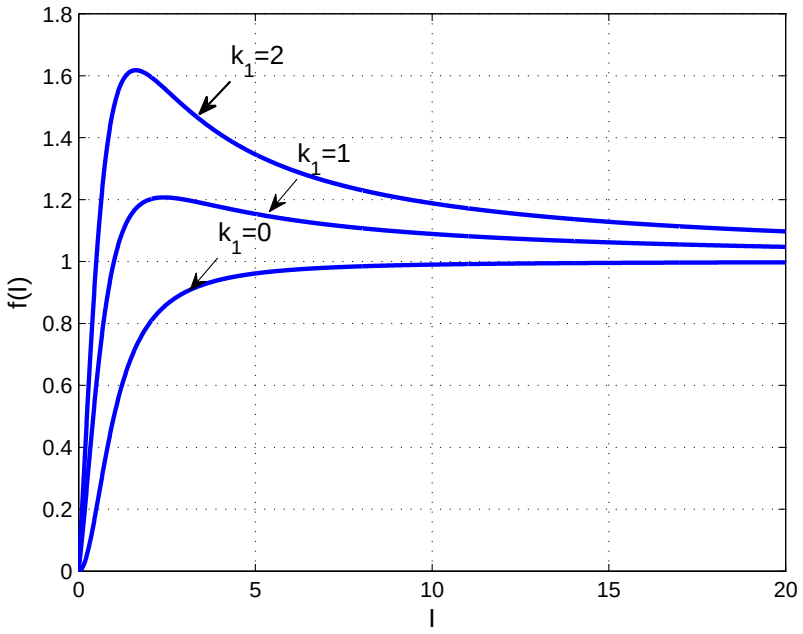

Figure 1. The incidence function $f(I) = \frac{k_1 I + k_2 I^2}{1+\alpha I^2}$ for $k_1 = 0$, $k_1 = 1$ and $k_1 = 2$.

This paper focuses on the detailed dynamics analysis of the following SIRS (Susceptible-Infected-Recovered-Susceptible) epidemic model:

$$\begin{cases} \frac{dS}{dt} = b - dS - \frac{k_1 I + k_2 I^2}{1 + \alpha I^2} S + \nu R, \\ \frac{dI}{dt} = \frac{k_1 I + k_2 I^2}{1 + \alpha I^2} S - (d + \gamma) I, \\ \frac{dR}{dt} = \gamma I - (d + \nu) R. \end{cases} \tag{2}$$

where the biological meaning of the parameters are the same as model (1), $(k_1 I + k_2 I^2)S$ measures linear and nonlinear hazards of infection, and $\frac{1}{1+\alpha I^2}$ describes the psychological effect. The basic reproduction number R_0 of the model is $\frac{bk_1}{d(d+\gamma)}$, and we will perform a qualitative dynamics analysis for model (2); it is shown that there may be two endemic

equilibria, which gives rise to the phenomenon of bistability (backward bifurcation) when parameters are lying in some region. We will investigate the local stability of these equilibria, classify the types of the equilibria, and discuss different kinds of bifurcation phenomena. A saddle-node bifurcation will be investigated for different perturbation parameters. Next, we will prove that the model can undergo Bogdanov–Takens bifurcation of, at most, codimension two, and the model with some specific parameters values can bifurcate at least three limit cycles through Hopf bifurcation of codimension three. Numerical simulations for these bifurcation phenomena will be presented to illustrate our theoretical results.

The organization of this paper is as follows. Existence and types of equilibria are presented in Section 2 by reducing the model to a two-dimensional system. In Section 3, we study the backward bifurcation, saddle-node bifurcation, and Bogdanov–Takens bifurcation of codimension two; Hopf bifurcation of codimension two; and Hopf bifurcation of codimension three. This paper ends with a brief conclusion and discussion of the results in Section 4.

2. Existence and Types of Equilibria

Note that the equation for the total population N is given by $\frac{dN}{dt} = b - dN$, where $N = S + I + R$. Since $N \to N_0 = \frac{b}{d}$ as $t \to \infty$, it is clear that:

$$\Omega = \{(S, I, R) : S, I, R \geq 0, S + I + R = N_0\}$$

is a positively invariant region for model (2). Hence, our study on the dynamics of model (2) is focused on the region Ω. Substituting $N_0 - I - R$ for S in model (2), we can obtain the following reduced model by eliminating S from the equations:

$$\begin{cases} \dfrac{dI}{dt} = \dfrac{k_1 I + k_2 I^2}{1 + \alpha I^2}(N_0 - I - R) - (d + \gamma)I, \\ \dfrac{dR}{dt} = \gamma I - (d + \nu)R. \end{cases} \tag{3}$$

Rescale model (3) by using $x = \sqrt{\frac{k_2}{d+\nu}}I, y = \sqrt{\frac{k_2}{d+\nu}}R, \theta = (d + \nu)t$, and let $\beta = \frac{k_1}{\sqrt{k_2(d+\nu)}}$, $p = \frac{d+\nu}{k_2}\alpha$, $m = \frac{d+\gamma}{d+\nu}$, $\Lambda = \sqrt{\frac{k_2}{d+\nu}}N_0, q = \frac{\gamma}{d+\nu}$. For simplicity, we still denote θ by t and obtain:

$$\begin{cases} \dfrac{dx}{dt} = \dfrac{x^2 + \beta x}{1 + px^2}(\Lambda - x - y) - mx, \\ \dfrac{dy}{dt} = qx - y. \end{cases} \tag{4}$$

It is evident that:

$$\beta \geq 0, \quad \Lambda, m, p, q > 0, \quad m > q, \tag{5}$$

and the positively invariant region of model (4) is:

$$D = \{(x, y) | x \geq 0, y \geq 0, x + y \leq \Lambda\}.$$

By using the next generation matrix [24], we derive the basic reproduction number $R_0 = \frac{\beta\Lambda}{m}$. Model (3) always has a equilibrium $E_0(0, 0)$. To find other equilibria of the model, we set:

$$\frac{x^2 + \beta x}{1 + px^2}(\Lambda - x - y) - mx = 0, \quad qx - y = 0, \tag{6}$$

and obtain:

$$(mp + q + 1)x^2 + (\beta q + \beta - \Lambda)x + m - \beta\Lambda = 0, \tag{7}$$

The discriminant of (7) is:

$$\Delta = (\Lambda - \beta - \beta q)^2 - 4(m - \beta\Lambda)(mp + q + 1).$$

From (6) and (7), there are at the utmost two endemic equilibria $E_1(x_1, y_1)$ and $E_2(x_2, y_2)$ in model (4), and they can merge into a unique endemic equilibrium $E_*(x_*, y_*)$, where:

$$\begin{aligned} x_1 &= \frac{\Lambda - \beta(1+q) - \sqrt{\Delta}}{2(1+q+mp)}, & y_1 &= qx_1, \\ x_2 &= \frac{\Lambda - \beta(1+q) + \sqrt{\Delta}}{2(1+q+mp)}, & y_2 &= qx_2, \\ x_* &= \frac{\Lambda - \beta(1+q)}{2(1+q+mp)}, & y_* &= qx_*. \end{aligned}$$

and:

$$x_1 + x_2 = \frac{\Lambda - \beta(1+q)}{1+q+mp}, \quad x_1 x_2 = \frac{m - \beta\Lambda}{1+q+mp}.$$

From $\Delta = 0$, we derive $p = \frac{(\Lambda-\beta-\beta q)^2 - 4(1+q)(m-\beta\Lambda)}{4m(m-\beta\Lambda)}$. Let:

$$p_* = \frac{(\Lambda - \beta - \beta q)^2 - 4(1+q)(m - \beta\Lambda)}{4m(m - \beta\Lambda)} \tag{8}$$

and $p_* > 0$, i.e.,

$$\beta\Lambda < m < \frac{(\Lambda - \beta - \beta q)^2}{4(1+q)} + \beta\Lambda. \tag{9}$$

Therefore, the following theorem is derived.

Lemma 1. *Under the condition of* (5)*, for model* (4)*, the equilibrium* $E_0(0,0)$ *always exists. Moreover,*
(I) Model (4) *has no endemic equilibria if and only if one of the following conditions holds:*
(I.1) $m \geq \beta\Lambda$ *and* $\Lambda \leq \beta + \beta q$*,*
(I.2) $\beta\Lambda < m < \frac{(\Lambda-\beta-\beta q)^2}{4(1+q)} + \beta\Lambda$, $\Lambda > \beta + \beta q$ *and* $p > p_*$*,*
(I.3) $m \geq \frac{(\Lambda-\beta-\beta q)^2}{4(1+q)} + \beta\Lambda$ *and* $\Lambda > \beta + \beta q$*.*
(II) There exists a unique endemic equilibrium $E_*(x_*, y_*)$ *if and only if* $\beta\Lambda < m < \frac{(\Lambda-\beta-\beta q)^2}{4(1+q)} + \beta\Lambda$, $\Lambda > \beta + \beta q$ *and* $p = p_*$*.*
(III) There exists a unique endemic equilibrium $E_2(x_2, y_2)$ *if and only if one of the following conditions holds:*
(III.1) $m = \beta\Lambda$ *and* $\Lambda > \beta + \beta q$*,*
(III.2) $m < \beta\Lambda$*.*
(IV) There exist two endemic equilibria $E_1(x_1, y_1)$ *and* $E_2(x_2, y_2)$ *if and only if:*
$\beta\Lambda < m < \frac{(\Lambda-\beta-\beta q)^2}{4(1+q)} + \beta\Lambda$, $\Lambda > \beta + \beta q$ *and* $p < p_*$*, where* $0 < x_1 < x_* < x_2$*.*

We denote a critical value $1 - \frac{(\Lambda-\beta-\beta q)^2}{4m(mp+q+1)}$ by R_c, and $0 < R_c < 1$. Moreover, $R_c > 0$ is equivalent to $p > p_0$, where $p_0 = \frac{(\Lambda-\beta-\beta q)^2 - 4m(q+1)}{4m^2}$. Note that $p > p_0$, i.e., $k_1 > k_1^*$, where

$$k_1^* = \frac{k_2\, b(d+v)}{d(\gamma+d+v)} - 2\,\frac{\sqrt{(d+\nu)(d+\gamma)(\gamma+d+\nu)k_2 + \alpha\,(d+\nu)^2(d+\gamma)^2}}{\gamma+d+\nu}.$$

Then, $\Delta = 0$ (i.e., $p = p_*$) is equivalent to $R_0 = R_c$. Hence, Lemma 1 can be written as the following result,

Theorem 1. *For model (4), there always exists a disease-free equilibrium E_0 with the conditions in (5) hold. Moreover,*
(1) If $R_0 < 1$ and
(1.1) $\Lambda \leq \beta q + \beta$, there are no endemic equilibria;
(1.2) $\Lambda > \beta q + \beta$, there exist two endemic equilibria E_1 and E_2 for $R_0 > R_c$ and when $p > p_0$ these two equilibria coalesce into E_* for $R_0 = R_c$.
(2) If $R_0 = 1$,
(2.1) $\Lambda \leq \beta q + \beta$, there are no endemic equilibria;
(2.2) $\Lambda > \beta q + \beta$, there exists a unique endemic equilibrium E_2;
(3) If $R_0 > 1$, there exists a unique endemic equilibrium E_2.

Now, let us study the types of these equilibria of model (4),

Theorem 2. *For model (4), the equilibrium $E_0(0,0)$ is:*
$R_0 < 1$: an attracting node;
$R_0 > 1$: a hyperbolic saddle;
$R_0 = 1$ and
• $\Lambda > \beta + \beta q$: a saddle-node of codimension 1;
• $\Lambda < \beta + \beta q$: a saddle-node of codimension 1;
• $\Lambda = \beta + \beta q$: a repelling semi-hyperbolic node of codimension 2.

Proof. For model (4), -1, and $m(R_0 - 1)$ are two eigenvalues of Jacobian at E_0. If $R_0 < 1$, E_0 is an attracting node. If $R_0 > 1$, E_0 is a hyperbolic saddle. If $R_0 = 1$, the second eigenvalue is zero. To determine the type of E_0, we linearize model (4) at E_0 and diagonalize the linear part, and on the center manifold, we have:

$$\begin{aligned} \frac{dX}{dt} =& (\Lambda - \beta\, q - \beta)X^2 + (\Lambda\, \beta\, p + 1 + q - \beta\, (\beta\, q - \Lambda + \beta)q)X^3 \\ &+ (\beta\, q - \Lambda + \beta)qX^4 + O(X^5). \end{aligned} \tag{10}$$

Hence, E_0 is a saddle-node of codimension one when $\Lambda \neq \beta + \beta q$ [25].

If $R_0 = 1$ and $\Lambda = \beta + \beta q$, model (10) becomes:

$$\frac{dX}{dt} = (1 + (\beta\, q + \beta)\beta\, p + q)X^3 + O(X^5). \tag{11}$$

Therefore, E_0 is a semi-hyperbolic repelling node. □

Theorem 3. *For model (4), the disease-free equilibrium E_0 is globally asymptotical stable if (I.1), or (I.2), or (I.3) of Lemma 1 (i.e., (1.1) or (2.1) of Theorem 1) holds.*

Proof. Note that $x = 0$ is an invariant line and D is positively invariant; by index theory [26], we can conclude that there are no nontrivial periodic orbits in $\mathbb{R}^2_+$ when model (4) has no endemic equilibria. □

Remark 1. *According to Theorem 1 and model (3), note that $\Lambda \leq \beta q + \beta$ is equivalent to $k_1 \geq k_{10}$, where $k_{10} = \frac{k_2\, b(d+v)}{d(\gamma+d+v)}$, which implies that when $\frac{k_1}{k_2}$, which measures the proportion of the linear over nonlinear hazards of infection, is larger than or equal to $\frac{b(d+v)}{d(\gamma+d+v)}$, and $R_0 \leq 1$, i.e., on average, an infected individual produces less than or equal to one new infected individual over the course of its infectious period, the infection cannot grow, that is, the disease cannot invade the population.*

3. Bifurcation Analysis

3.1. Backward Bifurcation and Saddle-Node Bifurcation

From Theorem 3, we know that E_0 is globally asymptotically stable when model (4) has no endemic equilibria. Next, we will discuss the bifurcation of model (4) with endemic equilibria.

Theorem 4. *For model (4), we choose R_0 as the bifurcation parameter.*
(1) When $R_0 = 1$, model (4) undergoes forward bifurcation if $\Lambda < \beta q + \beta$; model (4) undergoes backward bifurcation if $\Lambda > \beta q + \beta$; model (4) undergoes pitchfork bifurcation if $\Lambda = \beta q + \beta$.
(2) When $p > p_0$, model (4) undergoes saddle-node bifurcation when R_0 passes through R_c if $q \neq q_*$. When $R_0 = R_c$, E_0 is a saddle-node if $q \neq q_*$, and E_* is a cusp if $q = q_*$.

Proof. For the first statement (1), since R_0 can be seen as the function of the parameters β, Λ, and m, without loss of generality, we can choose m as the bifurcation parameter. Let $m = \beta\Lambda + \varepsilon$, and plug m into model (4), where $\varepsilon = 0$ corresponds to $R_0 = 1$. We linearize model (4) at E_0 and diagonalize the linear part. One can obtain the following reduced model on the center manifold by applying the center manifold theorem with the parameter ε.

$$\frac{dX}{dt} = -\varepsilon X - \left(\frac{(\Lambda-\beta)\varepsilon}{q} + \frac{\beta q - \Lambda + \beta}{q}\right)X^2 + O(X^3). \tag{12}$$

Denoting the right side of model (12) as $F(X, \varepsilon)$, we can derive:

$$F(0,0) = 0, \quad \frac{\partial F}{\partial X}(0,0) = 0, \quad \frac{\partial F}{\partial \varepsilon}(0,0) = 0,$$
$$\frac{\partial^2 F}{\partial X \partial \varepsilon}(0,0) = -1, \quad \frac{\partial^2 F}{\partial^2 X}(0,0) = 2\frac{\Lambda - \beta q - \beta}{q}.$$

Therefore, model (12) undergoes a transcritical bifurcation if $\Lambda \neq \beta q + \beta$ [27].

Since $\frac{\partial R_0}{\partial \varepsilon}|_{\varepsilon=0} = -\frac{1}{\beta\Lambda} < 0$, when R_0 crosses $R_0 = 1$, model (4) undergoes forward and backward bifurcation if $\Lambda < \beta q + \beta$ and $\Lambda > \beta q + \beta$, respectively.

If $\Lambda = \beta q + \beta$, model (12) on the center manifold becomes:

$$\begin{aligned}\frac{dX}{dt} = &-\varepsilon X - \beta\varepsilon X^2 - \frac{1}{q^2}\Big[\Big(\beta^2 pq + \beta^2 p + 1\Big)\varepsilon^2 - \Big(2\beta^2 pq + 2\beta^2 p + q + 2\Big)\varepsilon \\ &+\beta^2 pq + \beta^2 p + q + 1\Big]X^3 + O(X^4).\end{aligned} \tag{13}$$

For simplicity, we still denote the right side of model (13) as $F(X, \varepsilon)$, and derive:

$$F(0,0) = 0, \quad \frac{\partial F}{\partial X}(0,0) = 0, \quad \frac{\partial F}{\partial \varepsilon}(0,0) = 0, \quad \frac{\partial^2 F}{\partial X \partial \varepsilon}(0,0) = -1,$$
$$\frac{\partial^2 F}{\partial^2 X}(0,0) = 0, \quad \frac{\partial^3 F}{\partial^3 X}(0,0) = -\frac{(q+1)(\beta^2 p + 1)}{q^2} < 0.$$

Therefore, model (13) undergoes pitchfork bifurcation if $\Lambda = \beta q + \beta$ [27].

For $\varepsilon = 0$, model (12) and model (13) become model (10) and model (11), respectively.

The second statement (2) will be discussed in detail in the following part. □

Now, we study the dynamics of model (4) near the positive equilibria. The positive equilibria with coordinates (x, y) satisfy:

$$(x+\beta)(\Lambda - x - y) - m(1 + px^2) = 0, \quad y = qx,$$

and the Jacobian matrix of model (4) at the equilibrium $E(x, y)$ is:

$$J(E) = \begin{bmatrix} \frac{(\beta+2x)(-qx+\Lambda-x)}{px^2+1} - \frac{\beta x+x^2}{px^2+1} - \frac{2mpx^2}{px^2+1} - m & -\frac{\beta x+x^2}{px^2+1} \\ q & -1 \end{bmatrix}.$$

Then, the determinant of $J(E)$ is:

$$det(J(E)) = \frac{(3mp+3q+3)x^2 + (2\beta q - 2\Lambda + 2\beta)x - \beta\Lambda + m}{px^2+1},$$

and its sign is determined by:

$$S_D = (3mp+3q+3)x^2 + (2\beta q - 2\Lambda + 2\beta)x - \beta\Lambda + m. \tag{14}$$

Similarly, we obtain the trace of $J(E)$:

$$tr(J(E)) = \frac{(-3mp-p-2q-3)x^2 + (2\Lambda - \beta q - 2\beta)x + \beta\Lambda - m - 1}{px^2+1},$$

and its sign is determined by:

$$S_T = (-3mp-p-2q-3)x^2 + (-\beta q + 2\Lambda - 2\beta)x + \beta\Lambda - m - 1. \tag{15}$$

Set:

$$\begin{aligned} &A_1 = \Lambda - \beta q - \beta,\ A_2 = (q+1)(\Lambda\beta - 2m) + \Lambda^2,\ A_3 = \beta^2 q + \Lambda\beta + \beta^2 - 2m, \\ &C_1 = \Lambda^2 + \Lambda\beta - 2m,\ C_2 = \Lambda\beta + \beta^2 - 2m - 2, \\ &C_3 = (\Lambda-\beta)(2\Lambda\beta m + \Lambda\beta - 2m^2) + 2\Lambda,\ C_4 = \Lambda m - \beta m + \Lambda, \\ &C_5 = 2m^2 + 2m - 2\Lambda\beta m - \Lambda\beta,\ q_* = \frac{C_1}{C_5},\ q_{**} = \frac{C_1}{2m - \Lambda\beta}. \end{aligned}$$

Note that $C_1 > 0$ if $m < \frac{(\Lambda-\beta-\beta q)^2}{4(1+q)} + \beta\Lambda$; $C_2 < 0$ if $m > \beta\Lambda$ and $\Lambda > \beta + \beta q$; $C_4 > 0$ if $\Lambda > \beta + \beta q$; $C_5 > 0$ if $m > \beta\Lambda$. Then, there is the following theorem.

Theorem 5. *For model (4), when $\beta\Lambda < m < \frac{(\Lambda-\beta-\beta q)^2}{4(1+q)} + \beta\Lambda$, $\Lambda > \beta + \beta q$, $p = p_*$ and conditions in (5) hold, there is a unique positive equilibrium $E_*(x_*, y_*)$. Moreover,*
(I) if $q \neq q_*$, then $E_*(x_*, y_*)$ is a saddle-node, which is attracting (or repelling) if $q < q_*$ or $q > q_{**}$ (or $q_* < q < q_{**}$);
(II) if $q = q_*$, then $E_*(x_*, y_*)$ is a cusp of codimension two.

Proof. We plug $x = x_*$ and $p = p_*$ into S_D and S_T, and then obtain $S_D(x_*) = 0$ and:

$$S_T(x_*) = \frac{(2m^2 + 2m - 2\Lambda\beta m - \Lambda\beta)q - \Lambda^2 - \Lambda\beta + 2m}{(\Lambda\beta - 2m)q + \Lambda^2 + \Lambda\beta - 2m}.$$

Since $m > \beta\Lambda$, $C_5 > 0$ and $q_* < q_{**}$. Hence, $S_T(x_*) > 0$ if and only if $q_* < q < q_{**}$. Conversely, if $q < q_*$ or $q > q_{**}$, $S_T(x_*) < 0$.

Letting $X = x - x_*$, $Y = y - y_*$, $p = p_*$ and expanding the right-hand sides of model (4) as a Taylor series gives (X, Y are rewritten as x, y, respectively):

$$\begin{cases} \frac{dx}{dt} = -a_{11}qx + a_{11}y + a_{12}x^2 + a_{13}xy, \\ \frac{dy}{dt} = qx - y, \end{cases} \tag{16}$$

where:

$$a_{11} = \frac{2m(\Lambda\beta - m)}{(q+1)(\Lambda\beta - 2m) + \Lambda^2}, \quad a_{13} = -\frac{m\Lambda A_1^2}{A_2^2},$$
$$a_{12} = \frac{mA_1^2\Big(2\Big((q+1)^2\beta - (3q+1)\Lambda\Big)m + (q^2-1)\Lambda\beta^2 + 2\Lambda^2\beta q + \Lambda^3\Big)}{2A_2^2A_3}.$$

Letting $X = \frac{qx + a_{11}qy}{a_{11}q+1}$, $Y = \frac{-qx+y}{a_{11}q+1}$, we convert model (16) to (X, Y are rewritten as x, y, respectively):

$$\begin{cases} \frac{dx}{dt} = b_{11}x^2 + b_{12}xy + b_{13}y^2, \\ \frac{dy}{dt} = -b_{20}y + b_{21}x^2 + b_{22}xy + b_{23}y^2, \end{cases} \tag{17}$$

where:

$$b_{11} = \frac{A_1^3 m}{2qA_3A_2b_{20}}, \quad b_{12} = -\frac{mA_1^2b_{01}}{A_2^2A_3b_{20}}, \quad b_{13} = \frac{qmA_1^2a_{11}b_{02}}{2A_2^2A_3b_{20}},$$
$$b_{20} = a_{11}q + 1, \quad b_{21} = -\frac{A_1^3 m}{2qA_3A_2b_{20}}, \quad b_{22} = \frac{mA_1^2b_{01}}{A_2^2A_3b_{20}}, \quad b_{23} = -\frac{qmA_1^2a_{11}b_{02}}{2A_2^2A_3b_{20}},$$
$$b_{01} = (q+1)(1-a_{11})\Lambda\beta^2 + \Big(\Big(\Lambda^2 q + 2m(q+1)^2\Big)a_{11} + \Lambda^2\Big)\beta$$
$$+ \Big(\Lambda^3 - 2m(2q+1)\Lambda\Big)a_{11} - 2\Lambda m,$$
$$b_{02} = \Big(2\Lambda^2\beta q + \Lambda^3 + \Big(\beta^2q^2 - \beta^2 - 6mq - 2m\Big)\Lambda + 2\beta m(q+1)^2\Big)a_{11}$$
$$+ 2\Lambda^2\beta + \Big(2\beta^2 q + 2\beta^2 - 4m\Big)\Lambda.$$

On the center manifold, we have:

$$\frac{dx}{dt} = c_{11}x^2 + O(x^3),$$

where:

$$c_{11} = -\frac{mA_1^3}{2qC_5(q-q_*)A_3}.$$

Note that $A_3 < 0$ when $m > \beta\Lambda$, and then, $c_{11} \neq 0$. Hence, according to Theorems 7.1–7.3 in Zhang et al. [28], E_* is a saddle-node of codimension one. Then, we obtain the conclusion in (I).

For the second conclusion in (II), substituting $q = q_*$ into (16), we obtain:

$$\begin{cases} \frac{dx}{dt} = x - \frac{1}{d_{10}}y - d_{11}xy + d_{12}x^2, \\ \frac{dy}{dt} = d_{10}x - y, \end{cases} \tag{18}$$

where:

$$d_{11} = \frac{\Lambda C_4^2}{mC_1^2}, \quad d_{12} = \frac{(m(\beta-\Lambda)(\Lambda\beta - m) + \Lambda(\beta^2 - m - 2))C_4^2}{mC_2C_1C_5}, \quad d_{10} = \frac{C_1}{C_5}.$$

Next, let $X = d_{10}(1 - d_{10})x + d_{10}y$, $Y = d_{10}x - y$. We transform model (18) into (X, Y are rewritten as x, y, respectively):

$$\begin{cases} \dfrac{dx}{dt} = y + a_1x^2 + o(|(x,y)|^2), \\ \dfrac{dy}{dt} = d_1x^2 + e_1xy + +o(|(x,y)|^2), \end{cases} \tag{19}$$

where:

$$\begin{aligned} a_1 =& \frac{C_4^3(\Lambda\beta - m)(C_1 - C_5)}{C_2C_1^2mC_5}, \quad d_1 = -\frac{C_4^3(\Lambda\beta - m)}{C_2mC_1^2}, \quad e_1 = -\frac{C_4^2e_0}{C_2C_1^2mC_5}, \\ e_0 =& (2m+2)\beta\Lambda^4 + \Big(\Big(4m^2 - 2m\Big)\beta^2 + 8m^3 + 12m^2 + 4\,m\Big)\Lambda - 4\beta m^3 \\ &+ \Big((2m+3)\beta^2 - 2m^2 - 2m\Big)\Lambda^3 + \Big(\beta^3 - \Big(10m^2 + 14m + 2\Big)\beta\Big)\Lambda^2. \end{aligned}$$

Based on Remark 1 of section 2.13 in [26], we obtain the following equivalent model of (19) in a small neighborhood of $(0,0)$:

$$\begin{cases} \dfrac{dx}{dt} = y, \\ \dfrac{dy}{dt} = d_1x^2 + (e_1 + 2a_1)xy + o(|(x,y)|^3), \end{cases} \tag{20}$$

where:

$$e_1 + 2a_1 = -\frac{C_4^2C_3}{C_2mC_1^2}$$

Note that $d_1 < 0$ because of $C_2 < 0$.

By contradiction, we will prove $e_1 + 2a_1 \neq 0$(i.e., $C_3 \neq 0$). Setting $C_3 = 0$, then:

$$C_3 = (2\,\beta - 2\,\Lambda)m^2 + \Big(2\,\Lambda^2\beta - 2\,\Lambda\,\beta^2\Big)m + \Lambda^2\beta - \Lambda\,\beta^2 + 2\,\Lambda = 0.$$

We regard C_3 as a function of variable m and assume the real solutions of the function exist, that is, $m = m_{1,2}$ and it is evident that $m_1, m_2 < \beta\Lambda$. However $m > \beta\Lambda$ leads to a contradiction. In fact, $C_3 < 0$; hence, $e_1 + 2a_1 < 0$. Utilizing the results on page 167 of [26], $E_*(x_*, y_*)$ is a cusp of codimension two. □

Remark 2. *When $\beta = 0$ (i.e., $k_1 = 0$), model (4) becomes model (1.3) of Tang et al. [9]. From Theorem 5, we prove that model (4) undergoes Bogdanov–Takens bifurcation of codimension at most two near E∗, and it revises the corresponding results in [9].*

Remark 3. *From Theorem 4 and Theorem 5, when $k_1^* < k_1 < k_{10}$ (i.e., $\Lambda > \beta + \beta q$) for model (4), the disease will be eliminated if $R_0 < R_c$ (i.e., $p > p_*$ and $k_1 > k_1^*$), and if $R_0 = R_c$ (i.e., $p = p_*$ and $k_1 > k_1^*$), model (4) will present complex dynamics and these conditions are not enough to determine the dynamical behaviors, and the disease will persist or die out, which depends on the values of k_1 and k_2 (or q).*

Finally, we give the following the phase portraits via Matlab software (Figure 2).

Theorem 6. *If $\beta\Lambda < m < \frac{(\Lambda-\beta-\beta q)^2}{4(1+q)} + \beta\Lambda$, $\Lambda > \beta + \beta q$, $p < p_*$ and conditions in (5) hold, there are two endemic equilibria $E_1(x_1, y_1)$ and $E_2(x_2, y_2)$ for model (4). Furthermore, E_1 must be a hyperbolic saddle, and then, E_2 will be:*
(i) a stable hyperbolic focus (or node) if $S_T(x_2) < 0$; or
(ii) a weak focus (or a center) if $S_T(x_2) = 0$; or
(iii) an unstable hyperbolic focus (or node) if $S_T(x_2) > 0$.

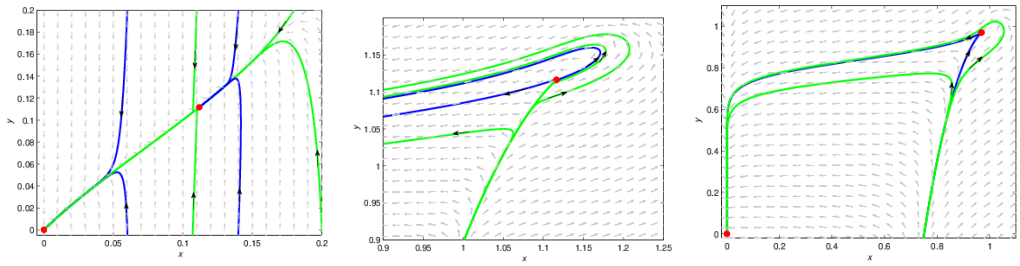

(**a**) (**b**) (**c**)

Figure 2. The phase diagram for model (4) with a unique endemic equilibrium: (**a**) an attracting saddle-node for $\beta = \frac{1}{5}, q = 1, m = 1, \Lambda = 4, p = \frac{71}{5}$; (**b**) a repelling saddle-node for $\beta = 1.7228$, $q = 1$, $m = 94.7654$, $\Lambda = 42.3881$, $p = 0.1629$; (**c**) a cusp of codimension two for $\beta = 0.5, q = 1.0019$, $m = 32$, $\Lambda = 33$, $p = 0.4535$.

Proof. For E_1 and E_2, the signs of $S_D(x_1)$, $S_D(x_2)$ and $S_T(x_2)$ are determined by S_D and S_T. By some simple calculations, we obtain:

$$S_D(x_1) = (3\,mp + 3\,q + 3){x_1}^2 + (2\,\beta\,q - 2\,\Lambda + 2\,\beta)x_1 + m - \beta\,\Lambda,$$

$$S_D(x_2) = (3\,mp + 3\,q + 3){x_2}^2 + (2\,\beta\,q - 2\,\Lambda + 2\,\beta)x_2 + m - \beta\,\Lambda.$$

Moreover, since x_1 and x_2 are two different positive roots of (7), we obtain:

$$\begin{aligned}
&(mp + q + 1)x_1^3 + (\beta q + \beta - \Lambda)x_1^2 + (m - \beta\Lambda)x_1 = 0,\\
&3(mp + q + 1){x_1}^2 + 2(\beta\,q - \Lambda + \beta)x_1 + m - \beta\,\Lambda < 0,\\
&(mp + q + 1)x_2^3 + (\beta q + \beta - \Lambda)x_2^2 + (m - \beta\Lambda)x_2 = 0,\\
&3(mp + q + 1){x_2}^2 + 2(\beta\,q - \Lambda + \beta)x_2 + m - \beta\,\Lambda > 0,
\end{aligned}$$

which yield $S_D(x_1) < 0$ and $S_D(x_2) > 0$. Then, these conclusions hold. □

Remark 4. *When $m = \beta\Lambda$, $\Lambda > \beta + \beta q$, or $m < \beta\Lambda$, model (4) has a unique positive equilibrium $E_2(x_2, y_2)$ and a disease-free equilibrium E_0. E_0 is a hyperbolic saddle or saddle-node, and the types and stability of E_2 are the same as Theorem 6. Moreover, from Theorem 6, when $R_0 > 1$ (i.e., $m < \beta\Lambda$), that is, each infected individual produces, on average, more than one new infection, or when $R_0 = 1$ and $\frac{k_1}{k_2} < \frac{b(d+v)}{d(\gamma+d+v)}$, which imply that when the proportion of the linear over nonlinear hazards of infection is less than $\frac{b(d+v)}{d(\gamma+d+v)}$, on average, each infected individual produces one new infection, and the disease will persist in the form of multiple periodic coexistent oscillations bifurcated from the equilibrium E_2.*

Remark 5. *$\Lambda > \beta + \beta q$ and $p < p_*$ are equivalent to $k_1 < k_{10}$ and $R_0 > R_c$, respectively. Hence, when $k_1^* < k_1 < k_{10}$, model (4) presents complex dynamics, and the disease will persist in the form of multiple periodic cycles if $R_0 > R_c$.*

3.2. Bogdanov–Takens Bifurcation

In this subsection, we will choose Λ and q as bifurcation parameters, and study Bogdanov–Takens bifurcation of codimension two for model (4). In fact, we have the following theorem:

Theorem 7. *When $\beta\Lambda < m < \frac{(\Lambda-\beta-\beta q)^2}{4(1+q)} + \beta\Lambda$, $\Lambda > \beta + \beta q$, $p = p_*$, $q = q_*$ and conditions in (5) hold, model (4) has a cusp $E_*(x_*, y_*)$ of codimension two (i.e., Bogdanov–Takens singularity). If we choose Λ and q as bifurcation parameters, Bogdanov–Takens bifurcation of codimension two in a small neighborhood of the unique positive equilibrium $E_*(x_*, y_*)$ occurs. Hence, there exists some*

parameter values such for which model (4) produces an unstable limit cycle, and model (4) produces an unstable homoclinic loop for some other parameter values.

Proof. We choose Λ and q as bifurcation parameters and consider:

$$\begin{cases} \dfrac{dx}{dt} = \dfrac{x^2+\beta x}{1+p_* x^2}(\Lambda+\lambda_1-x-y)-mx, \\ \dfrac{dy}{dt} = (q_*+\lambda_2)x-y, \end{cases} \tag{21}$$

where (λ_1, λ_2) is a parameter vector in near $(0,0)$. We focus on the phase portraits of model (21) with x and y lying near $E_*(x_*, y_*)$. Let $X = x - x_*$, $Y = y - y_*$. Then, we rewrite model (21) as (X, Y are rewritten as x, y, respectively):

$$\begin{cases} \dfrac{dx}{dt} = b_1 + b_2 x - \dfrac{1}{q_*}y + b_3 x^2 + b_4 xy + P_1(x, y, \lambda_1, \lambda_2), \\ \dfrac{dy}{dt} = b_5 + b_6 x - y, \end{cases} \tag{22}$$

where $P_1(x, y, \lambda_1, \lambda_2)$ is a C^∞ function at least of third order with respect to (x, y), and:

$$\begin{aligned} b_1 &= \frac{\lambda_1}{q_*}, \quad b_2 = \frac{\Lambda C_4^2 \lambda_1}{m C_1^2} + 1, \quad b_3 = \frac{C_4^2 b_{31}}{m^2 C_1^3 C_2 C_5}, \\ b_{32} &= \Lambda^4 \beta m + \Big(2\beta^2 m - m^2 + m + 2\Big)\Lambda^3 + \beta m\Big(\beta^2 - 8m - 7\Big)\Lambda^2 \\ &\quad + m^2\Big(\beta^2 + 6m + 6\Big)\Lambda - 2\beta m^3, \\ b_{31} &= C_4 b_{32}\lambda_1 - m\Big(m(\beta-\Lambda)(\Lambda\beta - m) + \Lambda(\beta^2 - m - 2)\Big)C_1^2, \\ b_4 &= -\frac{C_4^2 \Lambda}{m C_1^2}, \quad b_5 = -\frac{\lambda_2 C_5}{C_4}, \quad b_6 = \lambda_2 + q_*. \end{aligned}$$

Let $X = x$ and $Y = b_1 + b_2 x - \frac{1}{q_*}y + b_3 x^2 + b_4 xy + P_1(x, y, \lambda_1, \lambda_2)$ (we rewrite X, Y as x, y, respectively). Then, we obtain the following model:

$$\begin{cases} \dfrac{dx}{dt} = y, \\ \dfrac{dy}{dt} = c_1 + c_2 x + c_3 y + c_4 x^2 + c_5 xy + c_6 y^2 + Q_1(x, y, \lambda_1, \lambda_2), \end{cases} \tag{23}$$

where $Q_1(x, y, \lambda_1, \lambda_2)$ is a C^∞ function at least of third order with respect to (x, y) and:

$$\begin{aligned} c_1 &= \frac{b_1 q_* - b_5}{q_*}, \qquad c_2 = \frac{b_4 b_5 q_* + b_2 q_* - b_6}{q_*}, \qquad c_3 = 0, \\ c_4 &= -b_1 b_4^2 q_*^2 + b_4 b_6 + b_3, \quad c_5 = b_1 b_4^2 q_*^2 + b_4 b_2 q_* + 2b_3, \quad c_6 = -b_4 q_*. \end{aligned}$$

Next, let $dt = (1 - c_6 x)d\tau$; then, model (23) becomes (we still denote τ by t):

$$\begin{cases} \dfrac{dx}{dt} = y(1 - c_6 x), \\ \dfrac{dy}{dt} = (1 - c_6 x)\Big(c_1 + c_2 x + c_3 y + c_4 x^2 + c_5 xy + c_6 y^2 + Q_1(x, y, \lambda_1, \lambda_2)\Big). \end{cases} \tag{24}$$

Letting $X = x$, $Y = y(1 - c_6 x)$, and rewriting X, Y as x, y, respectively, we obtain:

$$\begin{cases} \dfrac{dx}{dt} = y, \\ \dfrac{dy}{dt} = d_1 + d_2 x + d_3 x^2 + d_4 xy + Q_2(x, y, \lambda_1, \lambda_2), \end{cases} \tag{25}$$

where $Q_2(x, y, \lambda_1, \lambda_2)$ is a $o(|(x, y)|^2)$ and:

$$d_1 = c_1, \quad d_2 = c_2 - 2c_1c_6, \quad d_3 = c_4 - 2c_2c_6 + c_1c_6^2, \quad d_4 = c_5.$$

Note that when $\lambda_1 = \lambda_2 = 0$, it is easy to derive that:

$$d_1 = 0, \quad d_2 = 0, \quad d_3 = \frac{C_4^3(\Lambda\beta - m)}{mC_1C_2C_5} < 0, \quad d_4 = \frac{C_4^2C_3}{mC_1C_2C_5} < 0.$$

Introducing a new time $t = \frac{d_4}{d_3}\tau$, we denote τ by t again. Moreover, performing a scaling by introducing the new variables:

$$X = \frac{d_4^2}{d_3}x, Y = \frac{d_4^3}{d_3^2}y,$$

and rewriting X, Y as x, y, respectively, we obtain:

$$\begin{cases} \dfrac{dx}{dt} = y, \\ \dfrac{dy}{dt} = \beta_1 + \beta_2 x + x^2 + xy + O(||(x, y)||^3), \end{cases} \tag{26}$$

where $\beta_1 = \frac{d_4^4}{d_3^3}d_1, \beta_2 = \frac{d_4^2}{d_3^2}d_2$. Since:

$$\left|\frac{\partial(\beta_1, \beta_2)}{\partial(\lambda_1, \lambda_2)}\right|_{(\lambda_1,\lambda_2)=0} = \frac{C_3^6}{q_* m(\Lambda\beta - m)^5 C_4^3 C_2 C_1^2} \neq 0,$$

for $\beta\Lambda < m < \frac{(\Lambda-\beta-\beta q)^2}{4(1+q)} + \beta\Lambda, \Lambda > \beta + \beta q_*$ and $q_* > 0$. The transformation is an invertible smooth change of parameters near the origin. Hence, model (26) undergoes Bogdanov–Takens bifurcation of codimension two when (λ_1, λ_2) changes in a small neighborhood of $(0, 0)$. □

Based on the study of [26], we get the bifurcation curves with second-order approximations (please refer to Supplementary Information at the end of the paper for more details or the link: http://doi.org/10.13140/RG.2.2.14757.17121 (accessed on 1 May 2023)).
(i) The saddle-node bifurcation curve is:

$$\begin{aligned} SN &= \{(\beta_1, \beta_2) | \beta_1 = 0, \beta_2 \neq 0\} \\ &= \Bigg\{ (\lambda_1, \lambda_2) | - \frac{C_3^2\Lambda\lambda_1}{m(\Lambda\beta - m)^2 C_1^2} + \frac{C_3^2(-2\Lambda\beta m + \Lambda^2 + 2m^2)\lambda_2}{mC_4^2(\Lambda\beta - m)^2 C_1 q_*} \\ &+ \frac{2\lambda_1^2 C_2 \Lambda^2 C_3}{(\Lambda\beta - m)^3 C_1^4 m^2}\left\{4\Lambda^4\beta m^2 - \ldots - 6\,\Lambda\, m^2\right\} \\ &- 2\,\frac{\lambda_2\,\lambda_1\,C_2\,\Lambda\,C_3}{(\Lambda\,\beta - m)^3 {C_4}^2 {C_1}^3 q_*\, m^2}\left\{4\,\Lambda^6\beta\, m^3 - \ldots - 6\Lambda^3 m^2\right\} \\ &+ \frac{2C_3^2(\Lambda^2 - 2\Lambda\beta m + 2m^2)\Lambda(2\Lambda^2 m + \Lambda^2 - 2m^2)C_2\lambda_2^2}{m^2 C_1^2 C_4^3(\Lambda\beta - m)^3 q_*^2} = 0, \beta_2 \neq 0 \Bigg\}. \end{aligned}$$

(ii) The Hopf bifurcation curve is:

$$\begin{aligned} H &= \{(\beta_1,\beta_2)|\beta_2 = \sqrt{-\beta_1}, \beta_1 < 0\} \\ &= \Bigg\{(\lambda_1,\lambda_2)| - \frac{C_3^4\lambda_1}{C_4 m {C_1}^2(\Lambda\beta - m)^3 C_2} + \frac{C_3^4\lambda_2}{q_* C_4^2 m C_1 (\Lambda\,\beta - m)^3 C_2} \\ &+ \frac{C_3^3\lambda_1^2}{C_2 C_1^4(\Lambda\beta - m)^4 m^2 C_4}\left(12\Lambda^6\beta^2m^2 - \ldots + 36\,\Lambda^2m^2\right) \\ &- \frac{C_3^3\lambda_1\lambda_2}{C_2 m^2 C_4^2(\Lambda\beta - m)^4 C_1^3 q_*}\left(22\,\Lambda^6\beta^2m^2 - \ldots + 44\,\Lambda^2m^2\right) \\ &+ \frac{C_3^4\lambda_2^2}{m^2 C_4^4(\Lambda\beta - m)^4 C_1^2 q_*^2}(6\Lambda^4m^2 - \ldots + 4\,m^4), \beta_1 < 0\Bigg\}. \end{aligned}$$

(iii) The homoclinic bifurcation curve is:

$$\begin{aligned} HL &= \{(\beta_1,\beta_2)|\beta_2 = \frac{5}{7}\sqrt{-\beta_1}, \beta_1 < 0\} \\ &= \Bigg\{(\lambda_1,\lambda_2)| - \frac{25{C_3}^4\lambda_1}{49 C_4 m {C_1}^2(\Lambda\beta - m)^3 C_2} + \frac{25{C_3}^4\lambda_2}{49 q_* {C_4}^2 m C_1(\Lambda\beta - m)^3 C_2} \\ &+ \frac{\lambda_1^2 C_3^3}{49 C_2 C_1^4(\Lambda\beta - m)^4 m^2 C_4}(348\,\Lambda^6\beta^2m^2 - \ldots + 900\Lambda^2m^2) \\ &- \frac{C_3^3\lambda_1\lambda_2}{49 C_2 C_4^2 m^2(\Lambda\beta - m)^4 C_1^3 q_*}(-992\,\Lambda^4 + \ldots + 716\Lambda^2m^2) \\ &+ \frac{C_3^4\lambda_2^2}{49 m^2 C_4^4(\Lambda\beta - m)^4 C_1^2 q_*^2}(150\Lambda^4m^2 - \ldots + 196\,m^4), \beta_1 < 0\Bigg\}. \end{aligned}$$

Next, the following bifurcation draft and phase graphs are shown via Matlab software.

From Figure 3, we show corresponding bifurcation draft and phase graphs for model (4) with $\beta = 0.5, m = 32$ and $\Lambda = 33$.

(a) From Figure 3a, it can be seen that the small neighborhood of the origin in the parameter (λ_1, λ_2)-plane is divided by bifurcation curves SN, H, and HL into four regions.

(b) When $(\lambda_1, \lambda_2) = (0, 0)$, the unique positive equilibrium is a cusp of codimension 2 (shown in Figure 2c).

(c) No equilibria exist (shown in Figure 3b) if the parameters are valued in region I.

(d) Entering from region I into region II, the parameters are valued on the saddle-node curve SN, the endemic equilibrium E_* emerges and it is a saddle-node.

(e) When the parameters cross SN into region II, the saddle-node turns into two positive equilibria through saddle-node bifurcation; one is an unstable node E_2 and the other is a saddle E_2 (shown in Figure 3c).

(f) Then, the node turns into a stable focus and loses stability when the parameters cross the Hopf bifurcation boundary H and an unstable limit cycle bifurcates from the subcritical Hopf bifurcation (shown in Figure 3d).

(g) When the parameters cross region III and lie on the curve HL, an unstable homoclinic cycle bifurcates from the homoclinic bifurcation (shown in Figure 3e).

(h) When the parameters cross III into region IV, the homoclinic cycle breaks up and the corresponding manifold eventually tends to the stable focus E_2 (shown in Figure 3f).

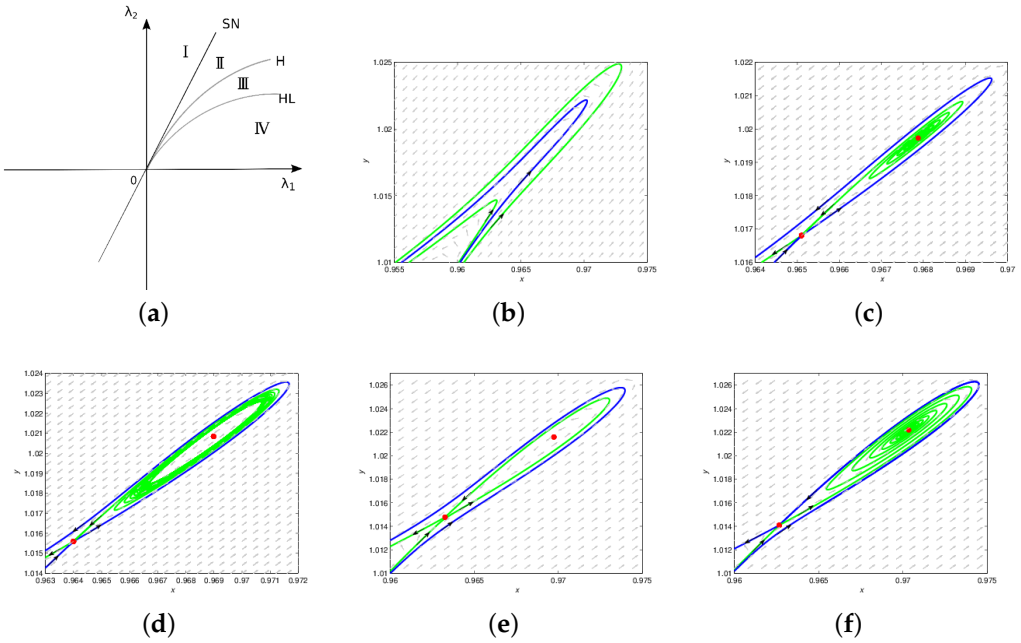

Figure 3. The bifurcation draft and phase graphs for model (4) with $\beta = 0.5, m = 32, \Lambda = 33$. (**a**) Bifurcation draft. (**b**) No endemic equilibria exist for model (4) with $(\lambda_1, \lambda_2) = (0.05, 0.0517)$, which are valued from region I. (**c**) An unstable focus E_2 and a saddle E_1 for model (4) with $(\lambda_1, \lambda_2) = (0.05, 0.5165)$, which are valued from region II. (**d**) An unstable limit cycle encloses a stable focus E_2 for model (4) with $(\lambda_1, \lambda_2) = (0.05, 0.516)$, which are valued from region III. (**e**) An unstable homoclinic loop for model (4) with $(\lambda_1, \lambda_2) = (0.05, 0.5155)$, which are valued on HL. (**f**) A stable focus E_2 and a saddle E_1 for model (4) with $(\lambda_1, \lambda_2) = (0.05, 0.515)$, which are valued from region IV.

3.3. Hopf Bifurcation of Codimension Two

From Theorem 6, Hopf bifurcation near $E_2(x_2, y_2)$ may occur. We obtain a reduced model (4) by the variable substitution:

$$\bar{x} = \frac{x}{x_2}, \quad \bar{y} = \frac{y}{y_2}, \quad \tau = x_2^2 t, \tag{27}$$

then, we transform model (4) into (we rewrite τ as t):

$$\begin{cases} \dfrac{d\bar{x}}{dt} = \dfrac{\bar{x}^2 + \frac{\beta}{x_2}\bar{x}}{1 + px_2^2\bar{x}^2}\left(\dfrac{\Lambda}{x_2} - \bar{x} - q\bar{y}\right) - \dfrac{m}{x_2^2}\bar{x}, \\ \dfrac{d\bar{y}}{dt} = \dfrac{1}{x_2^2}(\bar{x} - \bar{y}), \end{cases} \tag{28}$$

Substituting the following scaling for the parameters:

$$\bar{\beta} = \frac{\beta}{x_2}, \bar{\Lambda} = \frac{\Lambda}{x_2}, \bar{m} = \frac{m}{x_2^2}, a = \frac{1}{x_2^2}, \bar{p} = px_2^2, \bar{q} = q,$$

in model (28), and removing the bars, we have:

$$\begin{cases} \dfrac{dx}{dt} = \dfrac{x^2 + \beta x}{1 + px^2}(\Lambda - x - qy) - mx, \\ \dfrac{dy}{dt} = a(x - y). \end{cases} \tag{29}$$

There is an equilibrium $\bar{E}_2(1,1)$(i.e., $E_2(x_2, y_2)$ of model (4)), which makes the following equation true:

$$\Lambda = \frac{m(1+p)}{1+\beta} + q + 1.$$

Since $x_1 x_2 = \frac{m-\beta\Lambda}{mp+q+1}$ for model (4), then $\frac{x_1}{x_2} = \frac{\bar{m}-\bar{\beta}\bar{\Lambda}}{\bar{m}\bar{p}+\bar{q}+1}$ by (27), we remove the bars and obtain $m \geq \beta\Lambda$ and $q > m - mp - \beta\Lambda - 1$ due to $0 \leq \frac{x_1}{x_2} < 1$. Note that if $\Lambda = \frac{m(1+p)}{1+\beta} + q + 1$, then the conditions in (5) under above parameter scaling become:

$$\beta \geq 0, \quad p, q, m, a > 0, \quad \frac{m - pm(1+2\beta)}{(\beta+1)^2} - 1 < q < \frac{m}{a}, \quad m \geq \frac{\beta(\beta+1)(q+1)}{1-\beta p}. \tag{30}$$

Then, performing the change of time $dt = (1+px^2)(1+\beta)d\tau$ and plugging $\Lambda = \frac{m(1+p)}{1+\beta} + q + 1$ into (29), we have (rewrite τ as t):

$$\begin{cases} \frac{dx}{dt} = (1+\beta)x\Big(x(m+mp+(1+q-x-qy)(1+\beta)) - (1+px^2)m\Big), \\ \frac{dy}{dt} = (1+px^2)(1+\beta)a(x-y), \end{cases} \tag{31}$$

where m, p, q, β, a meet with (30). Actually, model (31) is topologically equivalent to model (29) in $\mathbb{R}^2 = \{(x,y) : x \geq 0, y \geq 0\}$; moreover, $1 + px^2 > 0$ holds for all $x \geq 0$. Next, we analyze the Hopf bifurcation near $\bar{E}_2(1,1)$ in model (31), which is equivalent to the Hopf bifurcation near $E_2(x_2, y_2)$ in model (4).

Theorem 8. *Under the conditions in* (30)*, there is an equilibrium* $\bar{E}_2(1,1)$ *for model* (31)*. Furthermore,*
(I) when $a < a_*$, $\bar{E}_2(1,1)$ *is an unstable hyperbolic node or focus;*
(II) when $a > a_*$, $\bar{E}_2(1,1)$ *is a locally asymptotically stable hyperbolic node or focus;*
(III) when $a = a_*$, $\bar{E}_2(1,1)$ *is a fine focus or center,*
where

$$a_* = \frac{m - (1+\beta)^2 - pm(1+2\beta)}{(\beta+1)(p+1)}.$$

Proof. The Jacobian matrix of model (31) at $\bar{E}_2(1,1)$ is:

$$J(\bar{E}_2(1,1)) = \begin{bmatrix} m - (1+\beta)^2 - pm(1+2\beta) & -(1+\beta)^2 q \\ a(1+p)(1+\beta) & -a(1+p)(1+\beta) \end{bmatrix}. \tag{32}$$

We obtain the determinant of $J(\bar{E}_2(1,1))$, which is:

$$det(J(\bar{E}_2)) = a(p+1)(1+\beta)[(q+1)(\beta+1)^2 + m(2\beta p + p - 1)].$$

Moreover, the trace is:

$$tr(J(\bar{E}_2)) = -(\beta+1)(p+1)a + m - (1+\beta)^2 - pm(1+2\beta).$$

Under the conditions in (30), we obtain that $det(J(\bar{E}_2)) > 0$ and $tr(J(\bar{E}_2)) = 0 (> 0 \text{ or } < 0)$ if $a = a_* (a < a_* \text{ or } a > a_*)$; hence, the conclusions hold. □

Note that Theorem 8 is true for $a_* > 0$, i.e.,

$$(\beta+1)^2 + m(2\beta p + p - 1) < 0, \text{ or } m > (1+\beta)^2,\ p < \frac{m - (1+\beta)^2}{m(1+2\beta)}.$$

Next, the case (III) of Theorem 8 is discussed, where Hopf bifurcation near $\bar{E}_2(1,1)$ of model (31) may occur when the following conditions are satisfied:

$$\begin{aligned} &a = a_*, \quad m > (1+\beta)^2, \quad p < \frac{m-(1+\beta)^2}{m(1+2\beta)}, \\ &\frac{m-pm(1+2\beta)}{(\beta+1)^2} - 1 < q < \frac{m}{a_*}, \quad m \geq \frac{\beta(\beta+1)(q+1)}{1-\beta p}. \end{aligned} \tag{33}$$

Firstly, the following transversality condition holds:

$$\frac{d}{da}(tr(J(\bar{E}_2)))|_{a=a_*} = -(\beta+1)(p+1) < 0.$$

Next, we evaluate the first Lyapunov coefficient l_1.

Let $X = x-1, Y = y-1$, and $a = a_*$. Then, model (31) becomes:

$$\begin{cases} \frac{dX}{dt} = &KX - q(1+\beta)^2 Y - q(1+\beta)(2+\beta)XY \\ &+ (K-(1+\beta)(1+mp))X^2 - (1+\beta)\Big(qX^2Y - (1+mp)X^3\Big), \\ \frac{dY}{dt} = &KX - KY - \frac{2pK}{p+1}XY + \frac{2pK}{p+1}X^2 - \frac{pK}{p+1}X^2Y + \frac{pK}{p+1}X^3. \end{cases} \tag{34}$$

where $K = -2\beta mp - \beta^2 - mp - 2\beta + m - 1$. Let $\omega = \sqrt{K(1+\beta)^2 q - K^2}$ and $X = 2\Phi - \frac{2\omega}{K}\Psi, Y = 2\Phi$; then, we obtain the following model:

$$\begin{cases} \frac{d\Phi}{dt} = &e_{11}\Psi + e_{12}\Phi\Psi + e_{13}\Psi^2 + e_{14}\Phi^2\Psi + e_{15}\Phi\Psi^2 + e_{16}\Psi^3, \\ \frac{d\Psi}{dt} = &e_{21}\Phi + e_{22}\Phi^2 + e_{23}\Phi\Psi + e_{24}\Psi^2 + e_{25}\Phi^2\Psi + e_{26}\Phi\Psi^2 + e_{27}\Phi^3 + e_{28}\Psi^3. \end{cases} \tag{35}$$

where:

$$\begin{aligned} e_{11} &= -\omega, e_{12} = -\frac{4p\omega}{p+1}, e_{13} = \frac{4p\omega^2}{K(p+1)}, e_{14} = -\frac{4p\omega}{p+1}, e_{15} = \frac{8p\omega^2}{K(p+1)}, \\ e_{16} &= -\frac{4p\omega^3}{K^2(p+1)}, e_{21} = \omega, e_{22} = \frac{2K}{\omega}((1+\beta)(\beta q + mp + 2q + 1) - K), \\ e_{23} &= \left(\frac{4K}{(p+1)} - 2(1+\beta)(\beta q + 2mp + 2q + 2)\right), \\ e_{24} &= \left(\frac{4p}{p+1} - 2 + \frac{2}{K}(\beta+1)(mp+1)\right)\omega, \\ e_{25} &= -4\left(\frac{pK}{p+1} + (\beta+1)(3mp + 2q + 3)\right), \\ e_{26} &= \left(\frac{4}{K}(\beta+1)(3mp + q + 3) + \frac{8p}{p+1}\right)\omega, \\ e_{27} &= \frac{4K}{\omega}(\beta+1)(mp+q+1), e_{28} = -\left(\frac{4p\omega^2}{K(p+1)} + \frac{4\omega^2}{K^2}(\beta+1)(mp+1)\right). \end{aligned}$$

According to Theorem 3.3 of [25] or formula (3.4.11) on Page 152 of [29], we obtain the first Lyapunov coefficient l_1 by Maple:

$$l_1 = -\frac{q(\beta+1)^2(q(c_1\,m + c_0) + d_2\,m^2 + d_1\,m + c_0)}{2\omega^3(p+1)^2} \tag{36}$$

where:

$$\begin{aligned}
c_1 =& \beta p^3 - 3(\beta+2)\left(2\beta^2+2\beta+1\right)p^2 + \left(2\beta^3+6\beta^2+9\beta+2\right)p + \beta,\\
c_0 =& (\beta+1)^3\left(\beta p^2 - 3\beta p - 3p + 1\right),\\
d_2 =& \beta p^4 - \left(16\,\beta^2+15\beta+6\right)p^3 + (15\beta+4)p^2 - (\beta+6)p,\\
d_1 =& \left(3\beta^3+3\beta^2+2\beta\right)p^3 - \left(12\beta^3+36\beta^2+27\beta+9\right)p^2\\
&+ \left(\beta^3+9\beta^2+18\beta+4\right)p - \beta - 3.
\end{aligned}$$

Let $q = q_0 = -\frac{d_2m^2+d_1m+c_0}{c_1m+c_0} > 0$, we obtain $l_1|_{q=q_0} = 0$. Therefore, based on the above caculations, we obtain the following result easily.

Theorem 9. *When* $(\beta, m, p) \in \{(\beta, m, p)|(d_2m^2 + d_1 + c_0)(c_1m + c_0) < 0\}$, *and the conditions in* (33) *hold, the following statements hold.*

(I) If $q > q_0$ *(i.e.,* $l_1 < 0$*), then model* (31) *generates supercritical Hopf bifurcation and a stable limit cycle bifurcates from* $\bar{E}_2(1,1)$.

(II) If $q < q_0$ *(i.e.,* $l_1 > 0$*), then model* (31) *generates subcritical Hopf bifurcation and an unstable limit cycle bifurcates from* $\bar{E}_2(1,1)$.

(III) If $q = q_0$ *(i.e.,* $l_1 = 0$*), then model* (31) *may generate degenerate Hopf bifurcation and multiple limit cycles may bifurcate from* $\bar{E}_2(1,1)$.

When $c_1, c_0 \neq 0$ *and* $m = -\frac{c_0}{c_1}$, *and the conditions in* (33) *hold, we have:*

(I) If $c_0 > 0$ *(i.e.,* $l_1 < 0$*), then model* (31) *generates supercritical Hopf bifurcation and a stable limit cycle bifurcates from* $\bar{E}_2(1,1)$*;*

(II) If $c_0 < 0$ *(i.e.,* $l_1 > 0$*), then model* (31) *generates subcritical Hopf bifurcation and an unstable limit cycle bifurcates from* $\bar{E}_2(1,1)$.

Proof. Through simple calculations, we obtain the following results.

Case 1, when $c_1 = 0$ for $\beta > 0$ and $p > 0$, it is evident that $c_0 \neq 0$, then $l_1 = 0$ if and only if $q = q_0$.

Case 2, when $c_1 \neq 0$ and $c_0 = 0$, then $l_1 = 0$ if and only if $q = q_0$.

Case 3, when $c_1, c_0 \neq 0$ and $c_1m + c_0 = 0$, we obtain $m = -\frac{c_0}{c_1}$, then:

$$d_2m^2 + d_1m + c_0 = \frac{\beta\,(p+1)^3(2\,\beta+p+3)c_0\,\left(\beta^2p+1\right)^2}{{c_1}^2} \neq 0.$$

Therefore, $l_1 \neq 0$ and $Sign(l_1) = Sign(-c_0)$.

Case 4, when $c_1 \neq 0$, $c_0 \neq 0$ and $c_1m + c_0 \neq 0$, then $l_1 = 0$ if and only if $q = q_0$. □

To numerically illustrate the results of the bifurcation analysis, with the help of Matlab software, we simulate an subcritical Hopf bifurcation with parameter values: $\beta = 0.4$, $m = 9$, $q = 6$, $p = 0.4$, $a = 0.2857$, one unstable limit cycle, bifurcated from the equilibrium $E_2(1,1)$ of model (29) with parameter α perturbed to $0.2857 + 0.03$, which is shown in Figure 4a. When the parameters become $\beta = 0.8$, $m = 9$, $q = 4$, $p = 0.1$, $a = 1.7273$, a stable limit cycle will arise from $\bar{E}_2(1,1)$ of model (29) with small perturbation -0.03 on α occurring (see Figure 4b). The coexistence of two limit cycles with the parameter values $\beta = 0.4$, $m = 3$, $q = 2.4269 + 0.1$, $p = 0.1$, $a = 0.3247 - 0.0002$ is shown in Figure 4c. The limit cycle with large amplitude is unstable, and the one with small amplitude is stable; both surround the stable endemic equilibrium $\bar{E}_2(1,1)$.

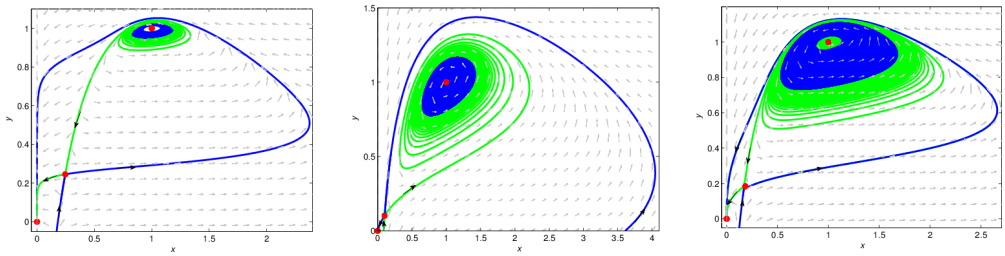

(**a**) (**b**) (**c**)

Figure 4. (**a**) An unstable limit cycle for model (31) with $\beta = 0.4, m = 9, q = 6, p = 0.4$, $a = 0.2857 + 0.03$. (**b**) A stable limit cycle for model (31) with $\beta = 0.8, m = 9, q = 4, p = 0.1$, $a = 1.7273 - 0.03$. (**c**) Two limit cycles for model (31) with $\beta = 0.4, m = 3, q = 2.4269 + 0.1$, $p = 0.1$, $a = 0.3247 - 0.0002$.

Remark 6. *From Figure 4a, there are three equilibria, a disease-free equilibrium, which is a stable node, and two endemic equilibria, where one is a saddle and the other is a stable focus. An unstable limit cycle encloses the focus. Therefore, the long-term disease dynamics may depend on the initial values of the populations, similar to Figure 4b,c.*

3.4. Hopf Bifurcation of Codimension Three

From Theorem 9, Hopf bifurcation of codimension three may occur for model (31) with $q = q_0$. In this section, we will study the phenomenon. To obtain the normal form of model (31), we make another transformation of $X = 2\Phi + \frac{2\omega}{K}\Psi$, $Y = 2\Phi$, and $\tau = \omega t$; then, system (34) becomes:

$$\begin{cases} \frac{d\Phi}{dt} = \Psi + h_{11}\Phi\Psi + h_{12}\Psi^2 + h_{13}\Phi^2\Psi + h_{14}\Phi\Psi^2 + h_{15}\Psi^3, \\ \frac{d\Psi}{dt} = -\Phi + h_{21}\Phi^2 + h_{22}\Phi\Psi + h_{23}\Psi^2 + h_{24}\Phi^2\Psi + h_{25}\Phi\Psi^2 + h_{26}\Phi^3 + h_{27}\Psi^3, \end{cases} \tag{37}$$

where:

$$\begin{aligned} h_{11} &= \frac{4p}{p+1}, \quad h_{12} = \frac{4p\omega}{K(p+1)}, \quad h_{13} = \frac{4p}{p+1}, \quad h_{14} = \frac{8p\omega}{K(p+1)}, \\ h_{15} &= \frac{4p\omega^2}{K^2(p+1)}, \quad h_{21} = \frac{2K}{\omega^2}(K - (1+\beta)(\beta q + mp + 2q + 1)), \\ h_{22} &= \frac{2}{\omega}\left(\frac{2K}{(p+1)} - (1+\beta)(\beta q + 2mp + 2q + 2)\right), \\ h_{23} &= 2 - \frac{4p}{p+1} - \frac{2}{K}(\beta+1)(mp+1), \\ h_{24} &= -\frac{4}{\omega}\left(\frac{pK}{p+1} + (\beta+1)(3mp + 2q + 3)\right), \\ h_{25} &= -\frac{4}{K}(\beta+1)(3mp + q + 3) - \frac{8p}{p+1}, \\ h_{26} &= -\frac{4K}{\omega^2}(\beta+1)(mp + q + 1), \quad h_{27} = -\frac{4p\omega}{K(p+1)} - \frac{4\omega}{K^2}(\beta+1)(mp+1). \end{aligned}$$

Next, applying the Maple program [28], we obtain the following focus values:

$$\begin{aligned}
f_1 =& \frac{1}{4{P_2}^3{P_1}^3}\Big({P_1}^4{P_2}^2{P_3}^2+{P_1}^2{P_2}^4{P_3}^2+5{P_1}^4{P_2}^2P_3+7{P_1}^2{P_2}^4P_3\\
&+{P_1}^2{P_2}^2P_3P_5\beta+2{P_2}^6P_3+{P_2}^4P_3P_5\beta+2{P_1}^4P_3P_4+8{P_1}^2{P_2}^4\\
&+3{P_1}^2{P_2}^2P_3P_4+2{P_1}^2{P_2}^2P_3P_5+2{P_1}^2{P_2}^2P_5\beta+8{P_2}^6+{P_2}^4P_3P_4\\
&+2{P_2}^4P_3P_5+6{P_2}^4P_5\beta+{P_2}^2{P_5}^2\beta^2+6{P_1}^4P_4+14{P_1}^2{P_2}^2P_4\\
&+8{P_1}^2{P_2}^2P_5+{P_1}^2P_4P_5\beta+8{P_2}^4P_4+12{P_2}^4P_5+3{P_2}^2P_4P_5\beta\\
&+4{P_2}^2{P_5}^2\beta+2{P_1}^2{P_4}^2+2{P_1}^2P_4P_5+2{P_2}^2{P_4}^2+6{P_2}^2P_4P_5+4{P_2}^2{P_5}^2\Big),\\
f_2 =& -\frac{1}{96P_2^7P_1^7}\Big(10{P_1}^{10}{P_2}^4{P_3}^4+55{P_1}^8{P_2}^6{P_3}^4+44{P_1}^6{P_2}^8{P_3}^4+\ldots\Big),\\
f_3 =& -\frac{1}{9216P_2^{11}P_1^{11}}\Big(1850{P_1}^{16}{P_2}^6{P_3}^6+3197{P_1}^{14}{P_2}^8{P_3}^6+\ldots\Big),
\end{aligned}$$

where $P_1=\frac{\omega}{\sqrt{K}}$, $P_2=\sqrt{K}$, $P_3=-\frac{4p}{p+1}$, $P_4=-2(1+\beta)(mp+1)$, $P_5=-2q(1+\beta)$, $f_i, i=1,2,3$, are lengthy polynomials in β, p, m, and q.

It is extremely difficult or impossible to solve $f_1=f_2=f_3=0$ for four parameters. We consider a specific case $p=\frac{1}{2(2\beta+1)}$ and $m=n_1(1+\beta)^2$ by introducing a new parameter $n_1>0$, which implies that p which describes the psychological effect is inversely proportional to β, which measures the infection force of the disease, and m, which represents the infection remove rate is proportional to β. Biologically, it means that the infection force of the disease is positively related to the psychological or inhibitory effect and the infection remove rate (including recovery rate and disease-related death rate). Under the assumptions, model (29) with parameters β and n_1 will exhibit Hopf bifurcation of codimension three. Let:

$$\begin{aligned}
z_1 =& -\Big(64\beta^6+432\beta^5+1084\beta^4+1353\beta^3+906\beta^2+313\beta+44\Big)n_1^3\\
&+\Big(256\beta^7+1984\beta^6+5712\beta^5+8060\beta^4+6044\beta^3+2348\beta^2+396\beta\\
&+12){n_1}^2+\Big(384\beta^4+1008\beta^3+1000\beta^2+440\beta+72\Big)n_1\\
&-8(\beta+1)\Big(4\beta^2-\beta-2\Big)(1+2\beta)^2,\\
z_2 =&\Big(32\beta^5+104\beta^4+120\beta^3+51\beta^2-\beta-4\Big)n_1-2\Big(4\beta^2+7\beta+2\Big)(1+2\beta)^3,\\
Q_3 =&\Big(576\beta^7+3272\beta^6+7122\beta^5+7500\beta^4+3736\beta^3+484\beta^2-250\beta-72\Big)n_1^2\\
&+\Big(256\beta^8+576\beta^7-1152\beta^6-5628\beta^5-9095\beta^4-8059\beta^3-4178\beta^2\\
&-1190\beta-144)n_1-512\beta^8-3456\beta^7-11072\beta^6-19968\beta^5-21188\beta^4\\
&-13370\beta^3-4884\beta^2-940\beta-72.
\end{aligned}$$

In fact, we have the following theorem.

Theorem 10. *If $q=q_0$, $z_1>0$, $z_2\geq 0$, $n_1>2$, and $Q_3=0$, model (29) (i.e., model (4)) undergoes a Hopf bifurcation of codimension three around the equilibrium $\bar{E}_2(1,1)$ (i.e., $E_2(x_2,y_2)$ in model (4)), three limit cycles bifurcate from $\bar{E}_2(1,1)$, and the outermost limit cycle is stable.*

Proof. From the assumptions $p=\frac{1}{2(2\beta+1)}$ and $m=n_1(1+\beta)^2$, we get:

$$a_*=\frac{(2\beta+1)(n_1-2)(1+\beta)}{3+4\beta},$$

where $n_1 > 2$ and $q > \frac{n_1}{2} - 1$; then:

$$P_1 = \frac{(1+\beta)}{2}\sqrt{4q-2n_1+4}, \quad P_2 = \frac{(1+\beta)}{2}\sqrt{2n_1-4}, \quad P_3 = -\frac{4}{3+4\beta},$$
$$P_4 = -(1+\beta)\left(\frac{n_1(1+\beta)^2}{2\beta+1}+2\right), \quad P_5 = -2q(1+\beta).$$

Then, the first focus value f_1 becomes:

$$f_1 = \frac{2q(Q_0 - 2(2\beta+1)Q_1 q)}{(2q+2-n_1)^{3/2}(n_1-2)^{3/2}(1+\beta)^2(2\beta+1)^2(3+4\beta)^2},$$

when $f_1 = 0$, we obtain $q = q_0 = \frac{Q_0}{2(2\beta+1)Q_1}$, where:

$$\begin{aligned} Q_0 =& \left(64\beta^4+304\beta^3+412\beta^2+225\beta+44\right)(\beta+1)^2 n_1^2 \\ & -2(2\beta+1)\left(16\beta^5+48\beta^4-17\beta^3-125\beta^2-104\beta-26\right)n_1 \\ & -4(\beta+1)\left(4\beta^2-\beta-2\right)(2\beta+1)^2, \\ Q_1 =& \left(32\beta^5+168\beta^4+260\beta^3+152\beta^2+23\beta-4\right)n_1 \\ & +16\beta^4+20\beta^3-6\beta^2-14\beta-4, \end{aligned}$$

the conditions of Hopf bifurcation in (33) become:

$$q_0 > 0, \quad \frac{z_1}{2(1+2\beta)Q_1(n_1-2)} > 0,$$
$$\frac{n_1(4\beta+3)}{2(1+2\beta)Q_1}\left(\beta^2+4\beta+2\right)Q_2 > 0, \quad \frac{n_1(\beta+1)}{(3\beta+2)Q_1}(\beta^2+4\beta+2)z_2 \geq 0,$$

that is:

$$Q_0 > 0,\ Q_1 > 0,\ z_1 > 0,\ z_2 \geq 0,\ n_1 > 2, \tag{38}$$

where:

$$Q_2 = 16\beta^3 + 16\beta^2 n_1 + 44\beta^2 + 23\beta n_1 + 34\beta + 8n_1 + 8.$$

When $f_1 = 0$, the second focus value f_2 becomes:

$$f_2 = -\frac{4Q_0^2 {n_1}^3(\beta^2+4\beta+2)^3 Q_3 Q_2^2}{3(2q_0+2-n_1)^{\frac{7}{2}}(n_1-2)^{\frac{5}{2}}(1+\beta)^3(2\beta+1)^5 {Q_1}^5}.$$

Hence, $f_2 = 0$ if and only if $Q_3 = 0$.

When $f_1 = 0$ (i.e., $q = q_0 = \frac{Q_0}{2(2\beta+1)Q_1}$), we obtain the third focus value f_3:

$$f_3 = \frac{1}{9}\frac{f_{33}\,{Q_0}^2}{(n_1-2)^{\frac{9}{2}}(\beta^2+4\beta+2)^{\frac{3}{2}}(2\beta+1)^{\frac{7}{2}}(1+\beta)^5(3+4\beta)^{\frac{13}{2}}Q_1^{\frac{5}{2}}Q_2^{\frac{7}{2}}n_1^{\frac{3}{2}}}.$$

where f_{33} is a redundant polynomial in variables β and n_1, which is given in the end of the paper (please refer to the link http://dx.doi.org/10.13140/RG.2.2.14757.17121 for more details) (accessed on 1 May 2023).

Evidently, the two polynomial equations $f_2 = f_3 = 0$ are equivalent to $Q_3 = f_{33} = 0$. Under the conditions in (38), $Q_3 = f_{33} = 0$ has no solutions for β and n_1 by simple calculation via Maple, and f_{33} is above Q_3 on the β-n_1 plane (see Figure 5). Hence, when $f_2 = 0$ (i.e., $Q_3 = 0$), it is easy to derive that the third focus value $f_3 < 0$ under the conditions in (38).

In conclusion, when the conditions in (38) hold, $Q_3 = 0$ should be the critical part of the black line which is under the red line on the right (see Figure 5), which makes $f_1 = f_2 = 0$ and $f_3 < 0$ true. Moreover, a simple calculation via Maple shows that on the black critical line:

$$det\left[\frac{\partial(f_1, f_2)}{\partial(\beta, n_1)}\right] = Q_4 \neq 0,$$

where Q_4 is given in the end of the paper (please refer to the link http://dx.doi.org/10.13140/RG.2.2.14757.17121 for more details) (accessed on 1 May 2023), which implies that if the values of parameters β and n_1 are on the black critical line, model (29) will exhibit Hopf bifurcation of codimension three and the outermost limit cycle is stable, since $f_3 < 0$. □

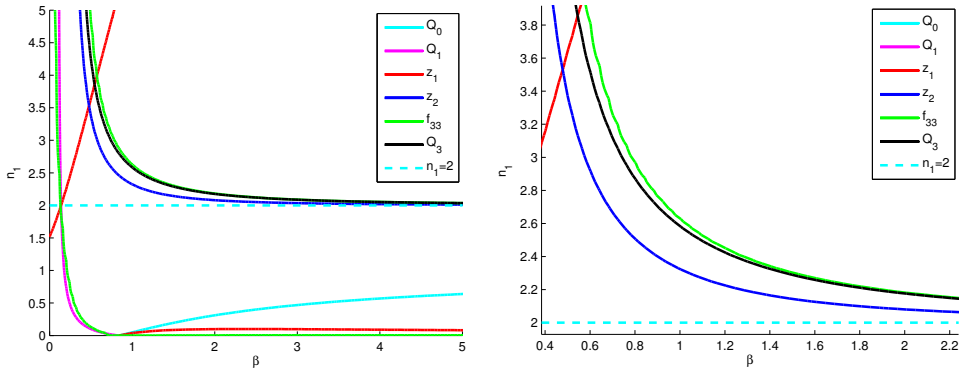

Figure 5. (**a**) Graphs of the regions on the β-n_1 plane. Under the conditions in (38), the black line under the red line on the right is the value range of parameters β and n_1, where Hopf bifurcation of codimension three will occur. (**b**) The value range is zoomed near $n_1 = 2$.

4. Conclusions and Discussions

In this paper, we focus on the bifurcation analysis of an SIRS epidemic model with a nonmonotone and saturated incidence rate. The incidence rate plays a key role in describing the spreading of infectious diseases and in producing the rich dynamics, including bistability (backward bifurcation) and periodicity. Based on research work conducted by pioneers, in 2019, a generalized nonmonotone and saturated incidence function $kI^2/(1 + \beta I + \alpha I^2)$ in model (1) was proposed by Lu et al. [20]; they considered that the incidence function, which described the infection force, should not be just monotonic, nonmonotonic, or saturated, but the combination of monotonicity, nonmonotonicity, and saturation properties. Considering the psychological and crowding effect, the incidence function seemed reasonable to describe the infection force of some specific infectious diseases. However, we have found that the basic reproduction number of model (1) with the incidence rate $kI^2S/(1 + \beta I + \alpha I^2)$ is zero, but the disease can still be persistent. Recently, Wang et al. [30] proved that model (1) can display bistable behaviors (backward bifurcation) with the threshold $\mathbb{R}_0 = \frac{bk}{\beta d(d+\gamma)}$, which is not the basic reproduction number of the model, and how to calculate the basic reproduction number of this model is still an open question. Hence, the incidence rate is difficult to understand. Moreover, the biological meaning of parameter β is undefined, and the condition $\beta > -2\sqrt{\alpha}$ is mandatory.

Hence, we propose a more reasonable incidence rate $\frac{k_1 I + k_2 I^2}{1+\alpha I^2} S$ with the combination of monotonicity, nonmonotonicity, and saturation properties. When $k_1 = 0$, the incidence function $f(I) = \frac{k_1 I + k_2 I^2}{1+\alpha I^2}$ becomes the saturated incidence function in [4], which increases monotonously and then goes to $\frac{k_2}{\alpha}$ as $I \to \infty$ (see Figure 1). When $k_1 > 0$, $f(I)$ increases firstly and then decreases to $\frac{k_2}{\alpha}$ as $I \to \infty$ (see Figure 1), which describes the fact that the infection force of some infectious diseases grows rapidly to the maximum as a new disease emerges or an old disease reemerges, and then trends to a value. We have carried out a qual-

itative analysis in this paper. The basic reproduction R_0 of model (2) is $\frac{bk_1}{d(d+\gamma)}$; we present that model (2) can undergo backward bifurcation with R_0 as the perturbation parameter if $\Lambda > \beta q + \beta$; backward bifurcation was proposed by Castillo-Chavez and Song [31] to illustrate that even if the basic reproduction number $R_0 < 1$, disease outbreaks are still possible. The backward bifurcation has further epidemiological implications by providing a threshold R_c; when $\Lambda > \beta q + \beta$, model (2) shows bistable behavior (endemic equilibrium E_2 and disease-free equilibrium are stable) if $R_c < R_0 < 1$, and the model has an unique endemic equilibrium E_2 and the disease-free equilibrium becomes unstable if $R_0 > 1$. Moreover, a saddle-node bifurcation at the threshold R_c has been studied. In our paper, there are the basic reproduction number R_0, threshold R_c, and critical values k_1^* and k_{10} of k_1, which measure the linear hazard of infection to determine the dynamic of model (4). Briefly, when $R_0 \leq 1$ and $\frac{k_1}{k_2}$, which measures the proportion of the linear over nonlinear hazards of infection, is larger than or equal to $\frac{b(d+v)}{d(\gamma+d+v)}$, the disease can be eliminated for all initial populations. When $R_0 > 1$ or $R_0 = 1$ and $\frac{k_1}{k_2} < \frac{b(d+v)}{d(\gamma+d+v)}$, the disease will persist in the form of multiple periodic coexistent oscillations bifurcated from the equilibrium E_2, or coexistent steady states for some initial populations. When $\frac{k_1}{k_2} < \frac{b(d+v)}{d(\gamma+d+v)}$, model (4) will present complex dynamics, including backward, saddle-node, and Hopf bifurcation, etc. In fact, when $k_1^* < k_1 < k_{10}$, the disease will disappear $R_0 < R_c$, but the disease will persist if $R_0 > R_c$, and for $R_0 = R_c$, these conditions are not enough to determine the dynamical behaviors, which implies the disease will persist or die out, which depends on the values of independent parameters k_1 and k_2 (or q), and it requires further assessment.

Moreover, we have proved that the model undergoes Bogdanov–Takens bifurcation of, at most, codimension two, which revises the results in [9] for $k_1 = 0$. Our studies on Hopf bifurcation of codimension two and three enrich the dynamics of SIRS epidemic models. In fact, it is difficult to take a complete analysis of Hopf bifurcation of codimension three. Assuming that the infection force of the disease measured by β is positively related to the psychological effect and the infection remove rate (including recovery rate and disease-related death rate), we obtain a complete qualitative analysis on Hopf bifurcation of codimension three for model (2). Next, we consider applying the model to practical problems, using the model for parameter estimation, and combining the actual data for numerical simulation and prediction analysis, so as to provide referable suggestions for the actual work department.

Author Contributions: Methodology, Y.Z.; Formal analysis, Y.Z.; Writing—original draft, Y.Z.; Writing—review & editing, C.L. All authors have read and agreed to the published version of the manuscript.

Funding: This work is financial supported by the Scientific Startup Foundation of Northwest A&F University (Z1090121104) and the National Natural Science Foundation of China (12201499).

Data Availability Statement: No data were used to support this study.

Conflicts of Interest: The authors declare that there are no conflict of interest regarding the publication of this paper.

References

1. Alexander, M.E.; Moghadas, S.M. Bifurcation analysis of an SIRS epidemic model with generalized incidence. *SIAM J. Appl. Math.* **2005**, *65*, 1794–1816. [CrossRef]
2. van den Driessche, P.; Watmough, J. A simple SIS epidemic model with a backward bifurcation. *J. Math. Biol.* **2000**, *40*, 525–540. [CrossRef]
3. Li, M.Y.; Liu, W.; Shan, C.; Yi, Y. Turning points and relaxation oscillation cycles in simple epidemic models. *SIAM J. Appl. Math.* **2016**, *76*, 663–687. [CrossRef]
4. Ruan, S.; Wang, W. Dynamical behavior of an epidemic model with a nonlinear incidence rate. *J. Differ. Equ.* **2003**, *188*, 135–163. [CrossRef]
5. Zhang, Y.; Zhou, Y.; Tang, B. Canard Phenomenon in an SIRS Epidemic Model with Nonlinear Incidence Rate. *Int. J. Bifurcat. Chao* **2020**, *30*, 2050073. [CrossRef]

6. Liu, W.; Hethcote, H.W.; Levin, S.A. Dynamical behavior of epidemiological models with nonlinear incidence rates. *J. Math. Biol.* **1987 25**, 359–380. [CrossRef]
7. Liu, W.; Levin, S.A.; Iwasa, Y. Influence of nonlinear incidence rates upon the behavior of SIRS epidemiological models. *J. Math. Biol.* **1986**, **23**, 187–204. [CrossRef] [PubMed]
8. Hethcote, H.W.; van den Driessche, P. Some epidemiological models with nonlinear incidence. *J. Math. Biol.* **1991**, *29*, 271–287. [CrossRef] [PubMed]
9. Tang, Y.; Huang, D.; Ruan, S.; Zhang, W. Coexistence of Limit Cycles and Homoclinic Loops in a SIRS Model with a Nonlinear Incidence Rate. *SIAM J. Appl. Math.* **2008**, *69*, 621–639. [CrossRef]
10. Hu, Z.; Bi, P.; Ma, W.; Ruan, S. Bifurcations of an SIRS epidemic model with nonlinear incidence rate. *Discret. Contin. Dyn. Syst. Ser. B* **2011**, *15*, 93–112. [CrossRef]
11. Kraemer, M.U.; Yang, C.H.; Gutierrez, B.; Wu, C.H.; Klein, B.; Pigott, D.M. The effect of human mobility and control measures on the COVID-19 epidemic in China. *Science* **2020**, *368*, 493–497. [CrossRef]
12. Novel Coronavirus Pneumonia Emergency Response Epidemiology Team, Vital Surveillances: The Epidemiological Characteristics of an Outbreak of 2019 Novel Coronavirus Diseases (COVID-19)-China, 2020. *China CDC Wkly.* 2020. Available online: http://weekly.chinacdc.cn/en/article/id/e53946e2-c6c4-41e9-9a9b-fea8db1a8f51 (accessed on 1 May 2023).
13. Tian, H.; Liu, Y.; Li, Y.; Wu, C.H.; Chen, B.; Kraemer, M.U.; Li, B.; Cai, J.; Xu, B.; Yang, Q.; et al. An investigation of transmission control measures during the first 50 days of the COVID-19 epidemic in China. *Science* **2020**, *368*, 638–642. [CrossRef]
14. Leung, G.M.; Lam, T.H.; Ho, L.M.; Ho, S.Y.; Chan, B.H.Y.; Wong, I.O.L.; Hedley, A.J. The impact of community psychological response on outbreak control for severe acute respiratory syndrome in Hong Kong. *J. Epidemiol. Commun. Health* **2003**, *57*, 857–863. [CrossRef] [PubMed]
15. Cheng, V.C.C.; Wong, S.C.; Chuang, V.W.M.; So, S.Y.C.; Chen, J.H.K.; Sridhar, S.; To, K.K.W.; Chan, J.F.W.; Hung, I.F.N.; Ho, P.L.; et al. The role of community-wide wearing of face mask for control of coronavirus disease 2019 (COVID-19) epidemic due to SARS-CoV-2. *J. Infect.* **2020**, *81*, 107–114. [CrossRef]
16. Zeng, Z.; Wu, T.; Lin, Z.; Luo, L.; Lin, Z.; Guan, W.; Liang, J.; Yu, M.; Guan, P.; He, W.; et al. Containment of SARS-CoV-2 Delta strain in Guangzhou, China by quarantine and social distancing: A modelling study. *Sci. Rep.* **2022**, *12*, 21096. [CrossRef] [PubMed]
17. Xiao, D.; Ruan, S. Global analysis of an epidemic model with a nonlinear incidence rate. *Math. Biosci.* **2007**, *208*, 419–429. [CrossRef]
18. Xiao, D.; Zhou, Y. Qualitative analysis of an epidemic model. *Can. Appl. Math. Q.* **2006**, *14*, 469–492.
19. Zhou, Y.; Xiao, D.; Li, Y. Bifurcations of an epidemic model with non-monotonic incidence rate of saturated mass action. *Chaos Soliton. Fract.* **2007**, *32*, 1903–1915. [CrossRef]
20. Lu, M.; Huang, J.C.; Ruan, S.G.; Yu, P. Bifurcation analysis of an SIRS epidemic model with a generalized nonmonotone and saturated incidence rate. *J. Differ. Equ.* **2019**, *267*, 1859–1898. [CrossRef] [PubMed]
21. Li, M.Y. *An Introduction to Mathematical Modeling of Infectious Diseases*; Springer: Edmonton, AB, Canada, 2018; pp. 31–32.
22. Li, J.; Zhou, Y.; Wu, J.; Ma, Z. Complex dynamics of a simple epidemic model with a nonlinear incidence. *Discret. Contin. Dyn. Syst. Ser. B* **2007**, *8*, 161–173. [CrossRef]
23. Li, C.; Li, J.; Ma, Z.; Zhu, H.,Canard phenomenon for an SIS epidemic model with nonlinear incidence. *J. Math. Anal. Appl.* **2014**, *8*, 987–1004. [CrossRef]
24. van den Driessche, P.; Watmough, J. Reproduction numbers and sub-threshold endemic equilibria for compartmental models of disease transmission. *Math. Biosci.* **2002**, *180*, 29–48. [CrossRef] [PubMed]
25. Kuznetsov, Y.A. *Elements of Applied Bifurcation Theory*, 3rd ed.; Springer: New York, NY, USA, 2004; p. 166.
26. Perko, L. *Differential Equations and Dynamical Systems*, 3rd ed.; Springer: New York, NY, USA, 2001.
27. Wiggins, S. *Introduction to Applied Nonlinear Dynamical Systems and Chaos*, 2nd ed.; Springer: New York, NY, USA, 2003.
28. Zhang, Z.; Ding, T.; Huang, W.; Dong, Z. *Qualitative Theory of Differential Equation*; Translations of Mathematical Monographsr: Providence, RI, USA, 1992.
29. Guckenheimer, J.; Holmes, P. *Nonlinear Oscillations, Dynamical Systems, and Bifurcations of Vector Fields*; Springer: New York, NY, USA, 1984; pp. 150–156.
30. Wang, S.; Bai, X.; Xu, F. Bistability in a SIRS Model with General Nonmonotone and Saturated Incidence Rate. *arXiv* **2019**, arXiv:1911.13002.
31. Castillo-Chavez, C.; Song, B. Dynamical Models of Tuberculosis and Their Applications. *Math. Biosci. Eng.* **2004**, *1*, 361. [CrossRef]